

Optimal UAV Relay Placement for Single User Capacity Maximization over Terrain with Obstacles

Junting Chen^{*†}, Urbashi Mitra[†], and David Gesbert[‡]

^{*}School of Science and Engineering, The Chinese University of Hong Kong, Shenzhen, Guangdong 518172, China

[†]Ming Hsieh Department of Electrical Engineering, University of Southern California, CA 90089, USA

[‡]Department of Communication Systems, EURECOM, Sophia-Antipolis 06410, France

Abstract—The problem of optimal unmanned aerial vehicle (UAV) placement in a constrained 3-D space to build a connection between a base station (BS) and a ground user is studied. The essential challenge is to avoid signal propagation blockage from the target user, while maintaining a good connection to the BS. Most existing work is based on stochastic terrain models, and hence the quality-of-service for a specific user was not guaranteed. In contrast, this paper seeks the optimal UAV position according to the actual terrain structure; to this end, a multi-segment propagation model is exploited. Using a novel angular coordinate transformation, a low complexity search algorithm is developed, where the search time is bounded for arbitrary terrain shapes. The paper also examines and proves the global optimality of the search algorithm. Numerical experiments are performed over a real-world urban topology and demonstrate superior performance gain of the UAV position found by the proposed algorithm.

Index Terms—UAV, relay communication, segmented propagation, optimization, cellular network

I. INTRODUCTION

This paper studies the application of low altitude small UAVs as flying relays to improve the communication between a BS and a ground user. An advantage of a UAV relay system is the ability to establish an improved propagation environment for a ground user, *e.g.*, via building line-of-sight (LOS) links. However, it is also very challenging to realize such a goal, because the terrain structure, such as buildings and vegetation, may be arbitrary. An off-line exhaustive search for the best UAV relay position may only work for areas that have already been finely explored, necessitating a large database. In general, optimizing the UAV position requires an efficient search strategy for the best BS-to-UAV and UAV-to-user propagation opportunities over generally unstructured landform.

Prior work bypassed these difficulties by using a flat-terrain model or a stochastic terrain model yielding a simplified problem formulation [1]–[6]. For example, [1]–[3] assumed LOS conditions regardless of the UAV and user positions. In [7], the probability distribution of LOS and non-line-of-sight (NLOS) conditions is modeled as a function of elevation angle from the user to the UAV. However, stochastic methods cannot exploit the best opportunity to serve a specific user in deep shadow. We will show that, in some application scenarios, significant performance improvement is possible

over the stochastic method towards the optimality, if the fine-grained terrain structure can be exploited.

The goal of the paper is to develop efficient algorithms for determining the optimal UAV relay position in 3-D for serving a single ground user. Even for such a simple network topology, it is non-trivial to find the optimal UAV position, because the terrain is usually irregular, blocking the UAV-to-user signals for certain UAV locations. When the terrain structure is known to the UAV, solving the UAV position optimization is computationally expensive as there is little structure to exploit, *e.g.*, lack of convexity. On the other hand, when there is no prior information of the terrain, the UAV needs to actively search for the best relay location, but the search is constrained by the limited time and energy resources in practice. Hence, an exhaustive search is prohibitive. Our prior work [8] studied a similar UAV positioning problem in 2-D by assuming a fixed UAV height. However, such a constraint strongly limits the potential gain of the UAV relay system. Moreover, the extension to 3-D without significantly increasing the complexity is also non-trivial.

In this paper, we exploit a nested multi-segment propagation model, discussed in Section II-A, to substantially reduce the search complexity. The model captures important features previously observed in [9], [10] from simulated data as well as real measurement data in an urban environment. Those features have also been leveraged (as a stochastic version) in [4]–[7] for air-to-ground channel modeling and UAV network optimization. Using the segmented propagation model, we show that it is sufficient to search on a 2-D plane parallel to the ground rather than in the entire 3-D space. An angular coordinate transformation technique is derived to exploit this property. As one of the key contributions of this paper, we develop a search strategy that is proven to converge to the globally optimal UAV position, while the worst-case search length is still linear to the dimension of the target area. We evaluate our strategy for an end-to-end capacity maximization application over a real-world urban city topology. Our strategy significantly outperforms the stochastic one, as expected.

II. SYSTEM MODEL

Consider a UAV equipped with radio devices that relays signals between a user located at $\mathbf{x}_u \in \mathbb{R}^3$ and a BS located at $\mathbf{x}_b \in \mathbb{R}^3$ as illustrated in Fig. 1 (a). Denote the UAV position

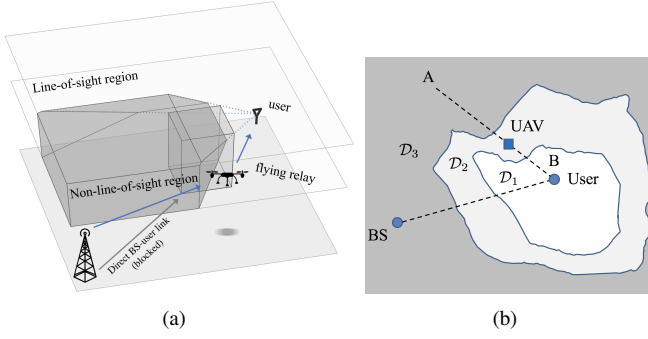


Figure 1. (a) Illustration of a communication network where a UAV establishes a LOS relay link to a user in the shadow of the BS coverage. (b) Geometric interpretation of the nested multi-segment propagation model from top view while fixing the height of the UAV.

as $\mathbf{x} = (x_1, x_2, x_3) \in \mathbb{R}^3$. Assume that user \mathbf{x}_u is located at ground level, $x_{u,3} = 0$, and the BS is placed on a high tower, $x_{b,3} = H_b > 0$, such that there is always LOS condition between the UAV and the BS. However, the UAV-to-user signal may be blocked by the terrain.

A. Segmented Propagation Model

Let $\mathbb{D} = \{\mathbf{x} : x_3 \geq H_{\min}\} \subseteq \mathbb{R}^3$ be the domain of all possible UAV positions \mathbf{x} . Typically, we require H_{\min} to be higher than all terrain structure. Consider a partition of \mathbb{D} into K disjoint segments according to the propagation environment around \mathbf{x}_u , i.e., $\mathbb{D} = \mathcal{D}_1 \cup \mathcal{D}_2 \cup \dots \cup \mathcal{D}_K$, where $\mathcal{D}_k \cap \mathcal{D}_j = \emptyset$, for $k \neq j$. Here, the *segments* or *regions* \mathcal{D}_k are the sets of UAV locations for which the UAV maintains a *degree- k* of LOS obstruction. In addition, as illustrated in Fig. 1 (b), the propagation segments \mathcal{D}_k are *nested*:

- 1) Increasing the altitude of the UAV will lower the degree of LOS obstruction, i.e., for any $(x_1, x_2, x_3) \in \mathcal{D}_k$ and $(x_1, x_2, x'_3) \in \mathcal{D}_j$, condition $x'_3 > x_3$ implies $j \leq k$;
- 2) The degree of LOS obstruction remains consistent when the UAV moves away from the user in a straight line, i.e., given any $\mathbf{x} \in \mathcal{D}_k$, $\mathbf{x}_u + \rho(\mathbf{x} - \mathbf{x}_u) \in \mathcal{D}_k$, $\forall \rho \geq 1$.

For example in a typical two segment case, segment \mathcal{D}_1 will correspond to the region of UAV positions where there is LOS condition to the user, and segment \mathcal{D}_2 to the NLOS condition.

B. Problem Formulation

The relay channel capacity of a decode-and-forward (DF) system can be shown to be given by $C_{\text{DF}} = \frac{1}{2} \min\{\log_2(1 + P_b g_{r,b} |a_{r,b}|^2), \log_2(1 + P_r g_{u,r} |a_{u,r}|^2)\}$ [11]. In an actual system, the averaged achievable data rate will depend on the average signal-to-noise ratio (SNR) $P_b g_{r,b}$ and $P_r g_{u,r}$ through a number of factors such as channel fading, channel coding schemes, modulation schemes, and rate adaptation strategy. As discussed in [12], this process can be abstracted in a discount factor κ , $0 < \kappa < 1$, resulting in a simplified but widely-used model for the effective SNR. Then, the relay capacity can be given by

$$C_{\text{DF}} = \frac{1}{2} \min\{\log_2(1 + \kappa P_b g_{r,b}), \log_2(1 + \kappa P_r g_{u,r}), r_{\max}\}. \quad (1)$$

Based on the analysis in [12], a typical choice of κ can be $\kappa = 0.5$. Here, we simply choose $r_{\max} = \infty$.

We assume that the network can use different radio access technologies depending on the propagation segments. For example, when the UAV-to-user link is in LOS, the network may choose to use wide-band millimeter wave (mmW) transmission, whereas, when it is in NLOS, the network may use a moderate bandwidth at the 2 GHz 3GPP band. As a result, the cost function f_k depends on the segment index k (the degree of signal obstruction):

$$f_k(d_u, d_b) = \frac{B_k}{2} \min\{\log_2(1 + \kappa P_b \beta_0 d_b^{-\alpha_0}), \log_2(1 + \kappa P_r \beta_k d_u^{-\alpha_k}), r_{\max}\}$$

for $k = 1, 2, \dots, K$, where B_k is the transmission bandwidth, $d_u(\mathbf{x}) \triangleq \|\mathbf{x} - \mathbf{x}_u\|_2$ is the UAV-to-user distance, and $d_b(\mathbf{x}) \triangleq \|\mathbf{x} - \mathbf{x}_b\|$ is the UAV-to-BS distance.

The UAV position optimization problem can be formulated as follows:

$$\begin{aligned} \mathcal{P} : \quad & \underset{\mathbf{x} \in \mathbb{R}^3}{\text{minimize}} && \sum_{k=1}^K f_k(d_u, d_b)(\mathbf{x}) \mathbb{I}\{\mathbf{x} \in \mathcal{D}_k\} \\ & \text{subject to} && H_{\min} \leq x_3 \leq H_{\max} \end{aligned}$$

where $\mathbb{I}\{A\}$ is an indicator function that satisfies $\mathbb{I}\{A\} = 1$ if event A is true and $\mathbb{I}\{A\} = 0$ otherwise, and $f(x, y)(\mathbf{x})$ is a short-hand notation of $f(x(\mathbf{x}), y(\mathbf{x}))$.

III. ALGORITHM DESIGN

The essential idea of the algorithm is to construct a 2-D search plane, such that by examining the propagation condition $\mathbb{I}\{\mathbf{x} \in \mathcal{D}_k\}$ over the search plane, the UAV can determine the cost in \mathcal{P} for the entire 3-D area.

A. Angular Coordinate System

First, we select a search altitude H_s satisfying $H_{\min} \leq H_s \leq H_{\max}$. Define a 3-D angular coordinate system with the user position \mathbf{x}_u being the origin. Define $\bar{\mathbf{x}}_s \in \mathbb{R}^2$ as the intersection point where the line segment, which joins \mathbf{x} and \mathbf{x}_u , intersects with the 2-D search plane $x_3 = H_s$. Next, we define the polar coordinates to represent $\bar{\mathbf{x}}_s$. Note that $\bar{\mathbf{x}}_s$ denotes the UAV position in the search phase. Specifically, let $\bar{\mathbf{x}}_b, \bar{\mathbf{x}}_u, \bar{\mathbf{x}} \in \mathbb{R}^2$, respectively, be the projected positions of $\mathbf{x}_b, \mathbf{x}_u$, and \mathbf{x} on the search plane $x_3 = H_s$, by simply dropping their third coordinates in the Cartesian system. Then, construct a polar coordinate system (ρ, θ) on the 2-D plane $x_3 = H_s$ using $\bar{\mathbf{x}}_u$ as the origin and $\mathbf{u} = (u_1, u_2) \triangleq (\bar{\mathbf{x}}_b - \bar{\mathbf{x}}_u) / \|\bar{\mathbf{x}}_b - \bar{\mathbf{x}}_u\|$ as the reference direction for $\theta = 0$, and based on that, compute the polar coordinates (ρ, θ) of the intersection point $\bar{\mathbf{x}}_s$. Finally, denoting $l = \|\mathbf{x} - \mathbf{x}_u\|_2$ as the distance from the UAV position $\mathbf{x} = (x_1, x_2, x_3)$ to the user, the UAV (x_1, x_2, x_3) is uniquely represented by the angular coordinates (l, ρ, θ) . The geometric interpretation of the transformation is illustrated in Fig. 2.

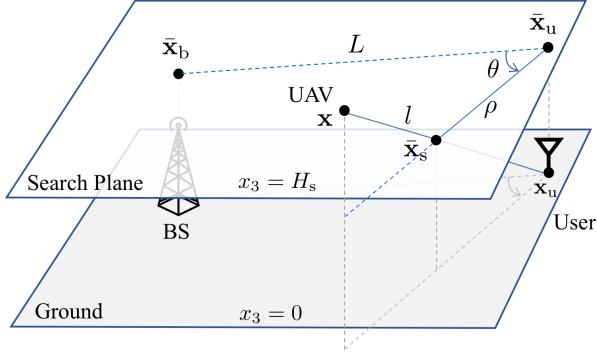


Figure 2. Geometric interpretation of the angular transformation.

Mathematically, transforming from (x_1, x_2, x_3) to (l, ρ, θ) we have:

$$l(\mathbf{x}) = \|\mathbf{x} - \mathbf{x}_u\|_2 \quad (2)$$

$$\rho(\mathbf{x}) = \frac{H_s}{x_3} \|\bar{\mathbf{x}} - \bar{\mathbf{x}}_u\|_2 \quad (3)$$

$$\theta(\mathbf{x}) = \text{sign}(z_2 u_1 - z_1 u_2) \cdot \arccos(\mathbf{z}^T \mathbf{u} / \|\mathbf{z}\|) \quad (4)$$

where $\mathbf{z} = (z_1, z_2) \triangleq \bar{\mathbf{x}} - \bar{\mathbf{x}}_u$, $\text{sign}(x) = 1$ if $x > 0$, and $\text{sign}(x) = -1$, otherwise.

In turn, transforming from (l, ρ, θ) to $\mathbf{x} = (x_1, x_2, x_3)$ yields:

$$\mathbf{x}(l, \rho, \theta) = l \frac{(\bar{\mathbf{x}}_s(\rho, \theta), H_s) - \mathbf{x}_u}{\|(\bar{\mathbf{x}}_s(\rho, \theta), H_s) - \mathbf{x}_u\|} \quad (5)$$

where $\bar{\mathbf{x}}_s(\rho, \theta) = \bar{\mathbf{x}}_u + \rho \mathbf{M}(\theta) \mathbf{u}$ and

$$\mathbf{M}(\theta) = \begin{bmatrix} \cos \theta & -\sin \theta \\ \sin \theta & \cos \theta \end{bmatrix} \quad (6)$$

is a rotation matrix.

B. Proxy Segment Cost on the Search Plane

Using the angular coordinate transformation (2)–(4), problem \mathcal{P} can be equivalently transformed into

$$\mathcal{P}' : \underset{\rho \geq 0, \theta \in (-\pi, \pi), l \in \mathcal{L}(\rho)}{\text{minimize}} \sum_{k=1}^K \tilde{f}_k(l, \rho, \theta) \mathbb{I}\{\mathbf{x}(l, \rho, \theta) \in \mathcal{D}_k\}$$

where $\tilde{f}_k(l, \rho, \theta) \triangleq f_k(d_u, d_b)(\mathbf{x}(l, \rho, \theta))$ and $\mathcal{L}(\rho) = \{l : \frac{H_{\min}}{H_s} \sqrt{\rho^2 + H_s^2} \leq l \leq \frac{H_{\max}}{H_s} \sqrt{\rho^2 + H_s^2}\}$.

Let $l_k^*(\rho, \theta)$ be the solution to the k th inner subproblem from \mathcal{P}' , i.e.,

$$l_k^*(\rho, \theta) \triangleq \arg \underset{l \in \mathcal{L}(\rho)}{\text{minimize}} \tilde{f}_k(l, \rho, \theta). \quad (7)$$

In fact, $l_k^*(\rho, \theta)$ can be computed efficiently according to the following proposition.

Proposition 1 (Unique Partial Minimizer I). *Under the angular coordinate transformation, $\tilde{f}_k(l, \rho, \theta)$ is strictly quasiconvex in l and admits a unique local minimizer $l_k^*(\rho, \theta)$ in $\mathcal{L}(\rho)$, i.e., $\partial \tilde{f}_k / \partial l < 0$ for $l < l_k^*(\rho, \theta)$ and $\partial \tilde{f}_k / \partial l > 0$ for $l > l_k^*(\rho, \theta)$.*

Defining the proxy cost for the k th segment evaluated on the search plane as

$$F_k(\rho, \theta) \triangleq \tilde{f}_k(l_k^*(\rho, \theta), \rho, \theta)$$

the 3-D search problem \mathcal{P}' is transformed into a 2-D problem:

$$\mathcal{P}'' : \underset{\rho \geq 0, -\pi \leq \theta \leq \pi}{\text{minimize}} F(\rho, \theta)$$

where $F(\rho, \theta) \triangleq \sum_{k=1}^K F_k(\rho, \theta) \mathbb{I}\{(\rho, \theta) \in \mathcal{P}_k\}$ and $\mathcal{P}_k \triangleq \{(\rho, \theta) : \mathbf{x}(l_k^*(\rho, \theta), \rho, \theta) \in \mathcal{D}_k\}$ is the k th propagation segment in the angular coordinate system.

C. Some Properties of the Transformation

We first show that one can infer the propagation condition in the entire 3-D area (hence obtain the partial solution $l^*(\rho, \theta)$ to \mathcal{P}') by exploring only over the 2-D search plane $x_3 = H_s$.

Proposition 2. *Given (ρ, θ) and some $l \in \mathcal{L}(\rho)$, if $\mathbf{x}(l, \rho, \theta) \in \mathcal{D}_k$ for some $k \in \{1, 2, \dots, K\}$, then $l^*(\rho, \theta) = l_k^*(\rho, \theta)$, where $l^*(\rho, \theta)$ is the solution to the inner subproblem*

$$\underset{l \in \mathcal{L}(\rho)}{\text{minimize}} \sum_{k=1}^K \tilde{f}_k(l, \rho, \theta) \mathbb{I}\{\mathbf{x}(l, \rho, \theta) \in \mathcal{D}_k\}$$

of \mathcal{P}' . In addition, $F(\rho, \theta) = F_k(\rho, \theta)$.

In addition, we find that there is no need to explore every point (ρ, θ) on the 2-D search plane, because one can *partially* infer the propagation condition from the nested property.

Proposition 3 (Nested Segments on the Search Plane). *The set $\{\mathcal{P}_k, k = 1, 2, \dots, K\}$ is a partition of $\mathbb{R}_+ \times [-\frac{\pi}{2}, \frac{\pi}{2})$ and satisfies the following condition: For any $(\rho, \theta) \in \mathcal{P}_k$ and $0 \leq \gamma \leq 1$, it holds that $(\gamma\rho, \theta) \in \mathcal{P}_j$, where $j \leq k$.*

Proposition 3 suggests that when the search position $\bar{\mathbf{x}}_s(\rho, \theta)$ moves towards the origin, i.e., the projected user position $\bar{\mathbf{x}}_u$ on the search plane, the propagation condition improves.

Finally, under the proposed transformation, the proxy segment cost $F_k(\rho, \theta)$ is quasiconvex in ρ , which guarantees a unique local minimum in ρ .

Proposition 4 (Unique Partial Minimizer II). *The proxy cost function $F_k(\rho, \theta)$ is strictly quasiconvex in ρ , and there is a unique local minimizer $\rho_k^*(\theta)$ of $F_k(\rho, \theta)$, i.e., $F_k(\rho_1, \theta) > F_k(\rho_2, \theta)$ for $\rho_1 < \rho_2 < \rho_k^*(\theta)$, and $F_k(\rho_3, \theta) < F_k(\rho_4, \theta)$ for $\rho_k^*(\theta) < \rho_3 < \rho_4$.*

D. The Algorithm

Following the observations found in Section III-C, we develop the search strategy in Algorithm 1.

E. Search Complexity and Global Optimality

We can show that the worst-case search length of Algorithm 1 is a linear function of the scale of the target area.

Theorem 1 (Maximum Trajectory Length). *The length of the search trajectory from Algorithm 1 is upper bounded by $(2.4K - 1.4) \frac{H_s}{H_{\min}} L$.*

Algorithm 1 Search Strategy on the Search Plane

Choose a step size $\delta > 0$. The search is carried out on a 2-D search plane $x_3 = H_s$ using the polar coordinates with $\bar{\mathbf{x}}_u$ as the origin and $\bar{\mathbf{x}}_b - \bar{\mathbf{x}}_u$ as the reference direction that defines $\theta = 0$.

- 1) **Search along $\theta = 0$:** Find the critical points ρ_k^0 , $k = 1, 2, \dots, K$, that minimizes $F_k(\rho, 0)$ subject to $(\rho, 0) \in \bigcup_{j=1}^k \mathcal{P}_j$. Initialize $F_{\min} = F_1(\rho_1^0, 0)$, $(\hat{\rho}, \hat{\theta}) = (\rho_1^0, 0)$, and $k = 1$.
- 2) **Search on the right branch:** Set $(\rho, \theta) \leftarrow (\rho_k^0, \delta/\rho_k^0)$.
- 3) Proceed according to the following two statuses
 - a) **Virtual LOS:** If $(\rho, \theta) \in \bigcup_{j=1}^k \mathcal{P}_j$, update

$$\rho \leftarrow \rho + \delta \quad (8)$$

If $F_k(\rho, \theta) < F_{\min}$, then update the record $F_{\min} \leftarrow F_k(\rho, \theta)$ and $(\hat{\rho}, \hat{\theta}) \leftarrow (\rho, \theta)$.

- b) **Virtual NLOS:** If $(\rho, \theta) \in \bigcup_{j=k+1}^K \tilde{\mathcal{P}}_j$, update

$$\rho \leftarrow \rho + \gamma, \theta \leftarrow \theta + \gamma \left(-\frac{\partial F_k}{\partial \theta} \right)^{-1} \frac{\partial F_k}{\partial \rho} \quad (9)$$

where $\gamma > 0$ is chosen such that the Euclidean norm of

$$\gamma \left[\mathbf{M}(\theta) \mathbf{u} + \rho \frac{d}{d\theta} \mathbf{M}(\theta) \mathbf{u} \left(-\frac{\partial F_k}{\partial \theta} \right)^{-1} \frac{\partial F_k}{\partial \rho} \right]$$

equals to the step size δ .

Repeat this step until either (i) $\rho \geq \frac{H_s}{H_{\min}} L \cos \theta$ or (ii) $\partial F_k(\rho, \theta)/\partial \rho \geq 0$, where $L \triangleq \|\bar{\mathbf{x}}_b - \bar{\mathbf{x}}_u\|_2$.

- 4) **Search on the left branch:** Set $(\rho, \theta) \leftarrow (\rho_k^0, -\delta/\rho_k^0)$. Repeat Step 3).
- 5) Let $k \leftarrow k + 1$. Repeat from Step 2) until $k > K - 1$.
- 6) If $F_K(\rho_K^0, 0) < F_{\min}$, then $F_{\min} \leftarrow F_K(\rho_K^0, 0)$ and $(\hat{\rho}, \hat{\theta}) \leftarrow (\rho_K^0, 0)$.

The optimal position is given by $\mathbf{x}(l^*(\hat{\rho}, \hat{\theta}), \hat{\rho}, \hat{\theta})$ from (5).

Proof: (Sketch) One can show that the iteration in Step 3 never decreases ρ and θ , and at the same time, the search region is bounded. Therefore, the search length is only linear in the scale of the target area. \square

Somewhat surprisingly, we can also show that, although the search has a linear length, the algorithm can find the global optimal position in 3-D under arbitrary propagation segments.

Consider a continuous-time algorithm trajectory $\mathbf{x}(t)$, which is obtained from Algorithm 1 using infinitesimal step size $\delta = \kappa dt$ at each infinitesimal time slot dt .

Theorem 2 (Global Optimality). *The process $(\hat{\rho}(t), \hat{\theta}(t))$ from Algorithm 1 converges to the globally optimal solution (ρ^*, θ^*) to problem \mathcal{P}'' in finite time $t = T < \infty$. In addition, $\mathbf{x}(l^*(\rho^*, \theta^*), \rho^*, \theta^*)$ from (5) is the globally optimal solution to problem \mathcal{P} .*

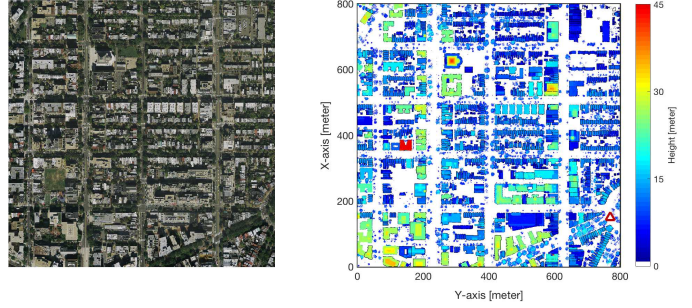


Figure 3. (Left) An orthoimagery of an 800 [m] \times 800 [m] area in Washington DC, USA. (Right) The corresponding elevation map of buildings and vegetation.

IV. NUMERICAL RESULTS

A. Propagation and Transmission Modeling

To simulate the segmented propagation environment, we use the geographical data captured in central Washington DC, USA, in 2013. Fig. 3 shows the orthoimagery of an 800 [m] \times 800 [m] area of interest and the corresponding elevation map. Building areas are designated by black polygons, whereas, the colored pixels outside the building areas represent the urban vegetation. The BS antenna is placed at (150, 770, 45) [m] to avoid any potential blockage of the UAV-to-BS link. The minimum UAV height is set as 45 meters to avoid collision with any building, and the maximum height is 120 meters to obey the US regulation.

We simulate three types of propagation conditions: The transceiver pair is in LOS condition, $k = 1$, if there is no building nor vegetation blocking the direct link from the transmitter to the receiver. It is in obstructed line-of-sight (OLOS) condition, $k = 2$, if there is only vegetation blockage of the direct link. Finally, it is in NLOS, $k = 3$, if there is a building that blocks the direct link.

When the UAV-to-user link is in LOS or OLOS, the network is transmitted in the mmW band with 500 MHz bandwidth, and the path loss is modeled as $61.4 + 20.0 \log_{10}(d)$ (LOS) or $81.4 + 20.0 \log_{10}(d)$ (OLOS) [13]. When the UAV-to-user link is in NLOS, the network uses the 3GPP band with 20 MHz bandwidth, and the path loss is modeled as $22.7 + 36.7 \log_{10}(d) + 26 \log_{10} f_c$, for $f_c = 2.5$ GHz [14]. The transmission powers are 23 dBm (BS) and 20 dBm (UAV), noise figure 7 dB.

B. Baseline Schemes

We evaluate the UAV placement method in Algorithm 1 with step size $\delta = 3$ meters, comparing with the following baseline schemes:

Direct BS-user link: The scheme transmits at the direct BS-user link, without the help of the UAV relay.

Statistical Method: The UAV is placed using a statistical method, where the UAV position is optimized according to the global statistics of the propagation conditions. Specifically, it solves \mathcal{P} by replacing the deterministic objective $f_k(d_u, d_b)(\mathbf{x}) \mathbb{I}\{\mathbf{x} \in \mathcal{D}_k\}$ by $f_k(d_u, d_b)p_k(\varphi(\mathbf{x}))$, where

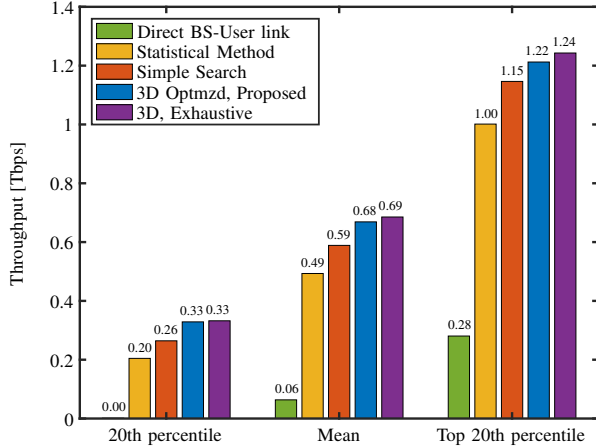


Figure 4. Throughput in terabits per second for different schemes.

$p_k(\varphi(\mathbf{x})) = \mathbb{P}\{\mathbf{x} \in \mathcal{D}_k | \varphi\}$ is the conditional probability of the UAV position \mathbf{x} belonging to the k th propagation segment given the elevation angle φ from the user position to \mathbf{x} . In the simulation, $p_k(\varphi)$ are obtained using empirical methods through a large amount of training user and UAV positions over the topology in Fig. 3.

Simple Method: This schemes performs an exhaustive search along the BS-user axis on the $x_3 = H_{\min}$ plane and finds the UAV position that minimizes the objective of \mathcal{P} .

Exhaustive Search: This schemes performs an exhaustive search over a 3-D lattice with 3 meter spacing. The lattice that achieves the minimum cost in \mathcal{P} is chosen as the optimal UAV position.

C. Results

Fig. 4 shows the end-to-end capacity evaluated over 10,000 user locations. First, it is observed that for the users in deep shadow (the 20th percentile) where the direct BS-user link is in complete outage, the proposed scheme can deliver 65% throughput gain over the statistical method. Second, the proposed schemes achieves a throughput almost as high as the one from exhaustive search, but the complexity is just linear as opposed to being cubic in the exhaustive search. Finally, a slight performance degradation (less than 2%) from the exhaustive search scheme is also observed. We conjecture that it is due to the 3 meter step size used in Algorithm 1, resulting in a cumulation of discretization error. To prove this conjecture, we reduce the step size to 1 meter in Algorithm 1, and find that the proposed scheme now achieves an average throughput of 0.69 Tbps (as the exhaustive scheme does). This numerically confirms that it finds the globally optimal solutions given a small enough step size.

V. CONCLUSIONS

This paper developed an efficient search algorithm to find the globally optimal UAV position for establishing the best relay link between a BS and a user, where the UAV-to-user

link is likely blocked by terrain obstacles. As opposed to statistical methods, the algorithm adapts to the actual terrain structure. The algorithm was developed based on a segmented propagation model and an angular coordinate transformation. It has been proven to find the globally optimal UAV position in 3-D, while the worst case search length is bounded by a linear function of the BS-user distance. The results were numerically confirmed experiments over a real terrain topology, where the proposed method demonstrate substantial performance gain over methods based on stochastic terrain models.

ACKNOWLEDGMENTS

This research has been funded, in part, by one or more of the following grants: ONR N00014-15-1-2550, NSF CNS-1213128, NSF CCF-1718560, NSF CCF-1410009, NSF CPS-1446901, AFOSR FA9550-12-1-0215, and ERC under the European Union Horizon 2020 research and innovation program (Agreement no. 670896).

REFERENCES

- [1] J. Lyu, Y. Zeng, R. Zhang, and T. J. Lim, "Placement optimization of UAV-mounted mobile base stations," *IEEE Commun. Lett.*, vol. 21, no. 3, pp. 604–607, 2017.
- [2] V. V. Chetlur and H. S. Dhillon, "Downlink coverage analysis for a finite 3-D wireless network of unmanned aerial vehicles," *IEEE Trans. Commun.*, vol. 65, no. 10, pp. 4543–4558, 2017.
- [3] Y. Zeng, R. Zhang, and T. J. Lim, "Throughput maximization for UAV-enabled mobile relaying systems," *IEEE Trans. Commun.*, vol. 64, no. 12, pp. 4983–4996, 2016.
- [4] A. Hourani, K. Sithampanathan, and S. Lardner, "Optimal LAP altitude for maximum coverage," *IEEE Commun. Lett.*, no. 99, pp. 1–4, 2014.
- [5] M. Mozaffari, W. Saad, M. Bennis, and M. Debbah, "Efficient deployment of multiple unmanned aerial vehicles for optimal wireless coverage," *IEEE Commun. Lett.*, vol. 20, no. 8, 2016.
- [6] M. Alzenad, A. El-Keyi, F. Lagum, and H. Yanikomeroglu, "3-D placement of an unmanned aerial vehicle base station (UAV-BS) for energy-efficient maximal coverage," *IEEE Wireless Commun. Lett.*, vol. 6, no. 4, pp. 434–437, 2017.
- [7] A. Al-Hourani, S. Kandeepan, and A. Jamalipour, "Modeling air-to-ground path loss for low altitude platforms in urban environments," in *Proc. IEEE Global Telecomm. Conf.*, 2014, pp. 2898–2904.
- [8] J. Chen and D. Gesbert, "Efficient local map search algorithms for the placement of flying relays," 2017, under review, preprint arXiv:1801.03595.
- [9] Q. Feng, J. McGeehan, E. K. Tameh, and A. R. Nix, "Path loss models for air-to-ground radio channels in urban environments," in *Proc. IEEE Semiannual Veh. Technol. Conf.*, vol. 6, 2006, pp. 2901–2905.
- [10] K. T. Herring, J. W. Holloway, D. H. Staelin, and D. W. Bliss, "Path-loss characteristics of urban wireless channels," *IEEE Trans. on Antennas and Propagation*, vol. 58, no. 1, pp. 171–177, 2010.
- [11] J. N. Laneman, D. N. Tse, and G. W. Wornell, "Cooperative diversity in wireless networks: Efficient protocols and outage behavior," *IEEE Trans. Inf. Theory*, vol. 50, no. 12, pp. 3062–3080, 2004.
- [12] P. Mogensen, W. Na, I. Z. Kovács, F. Frederiksen, A. Pokhariyal, K. I. Pedersen, T. Kolding, K. Hugel, and M. Kuusela, "LTE capacity compared to the Shannon bound," in *IEEE Veh. Technol. Conf.*, 2007, pp. 1234–1238.
- [13] M. R. Akdeniz, Y. Liu, M. K. Samimi, S. Sun, S. Rangan, T. S. Rappaport, and E. Erkip, "Millimeter wave channel modeling and cellular capacity evaluation," *IEEE J. Sel. Areas Commun.*, vol. 32, no. 6, pp. 1164–1179, 2014.
- [14] "Technical specification group radio access network; evolved universal terrestrial radio access (e-utra); further advancements for e-utra physical layer aspects;" 3GPP TR 36.814, Tech. Rep., 2010. [Online]. Available: <http://www.3gpp.org>